



Geothermal potential assessment for a low carbon strategy: A new systematic approach applied in southern Italy



E. Trumpy^{a, *}, S. Botteghi^a, F. Caiozzi^a, A. Donato^a, G. Gola^a, D. Montanari^a,
M.P.D. Pluymaekers^b, A. Santilano^a, J.D. van Wees^{b, c}, A. Manzella^a

^a Institute of Geosciences and Earth Resources – National Research Council, Via Moruzzi 1, 56124 Pisa, Italy

^b TNO – Geological Survey of the Netherlands, P.O. Box 80015, 3508 TA Utrecht, The Netherlands

^c Utrecht University, Faculty of Geosciences, P.O. Box 80021, 3508 TA Utrecht, The Netherlands

ARTICLE INFO

Article history:

Received 14 December 2015

Received in revised form

15 February 2016

Accepted 24 February 2016

Available online 21 March 2016

Keywords:

Geothermal maps
Potential assessment
Emission reduction
Power production
District heating

ABSTRACT

In this study a new approach to geothermal potential assessment was set up and applied in four regions in southern Italy. Our procedure, VIGORThermoGIS, relies on the volume method of assessment and uses a 3D model of the subsurface to integrate thermal, geological and petro-physical data. The method thus produces 2D geothermal potential maps for three different uses: district heating, district heating and cooling, and electrical power production. Our study focused on carbonate reservoirs, which usually present an excellent natural permeability and important geothermal gradients at depth. Our computations were possible thanks to the large quantity of data available from hydrocarbon exploration that largely investigate deep-seated reservoirs. Based on geothermal potential available for power production we estimate the contribution of the geothermal energy in the CO₂ emissions reduction in the study regions. Moreover policy makers as well as investors can use our maps to establish new policies and to locate the most promising places for geothermal development, in line with the international low carbon strategy.

© 2016 Elsevier Ltd. All rights reserved.

1. Introduction

Economic development is strongly correlated with increasing energy use and the related rise of GHG (greenhouse gas) emissions. The use of RE (renewable energy) can help decouple this correlation, thus contributing to sustainable development.

The ratified Kyoto Protocol in 2005 [1], establishes the future target GHG cap emissions for different countries in the future, compared to 1990 levels, resulting in GHG emission reductions by 20% in 2020 and 50% in 2050 respectively.

To meet these challenging targets, many international organizations and governments are promoting the use of renewable energy in the private and public sectors.

Geothermal energy, the renewable with the most secure base-load and low GHG emissions [2], supplies heat for direct use and energy for power production. In the last century, heat from the Earth's interior has been used in 25 countries for electricity

production, with an estimate of 73.5 TWh/yr of supplied energy provided in 2015 [3]. In addition 82 countries are using the direct heat, for heating and cooling, generating 163.2 TWh/yr of thermal energy to 2015, including GHP (geothermal heat pump) applications [4].

Geothermal energy can play a significant role in the abatement of GHG emissions, yielding up to 4% of future energy consumption (power and heat) [2,5].

Most of the actual production is deployed from hydrothermal reservoirs, made of underground fluid-filled rocks where fluids are heated by the natural heat of the earth and are brought to the surface by means of wells.

The known high temperature (above 180 °C) hydrothermal resources occur only in few places in the world, usually volcanic and magmatic areas. However, the optimization of technologies able to co-produce power and heat from hydrothermal systems of medium temperature (usually in the range 110–180 °C) has produced an impressive increase of geothermal plants from medium-temperature resources in non-volcanic areas.

Geothermal energy can be developed economically and at low risk, when targeting naturally permeable reservoirs, which have

* Corresponding author.

E-mail address: e.trumpy@igg.cnr.it (E. Trumpy).

been explored (and exploited) extensively over the past decades by the hydrocarbon industry. This is clearly demonstrated in the Netherlands, where over 10 geothermal heat plants have been developed in the last 10 years in sandstone reservoirs at 2–3 km depths, thanks also to public access to data and subsurface models [6].

Apart from sandstone, (fractured) carbonate reservoirs have considerable geothermal potential [7,8,9], as they have excellent natural permeability for geothermal development and the cogeneration of heat and power from reservoirs at great depths (see research projects such as GeoMol [10], and deployment projects such as Traunreut [11], Taufkirchen [12], Unterhaching [13]).

2. Objective

In this paper we highlight the significance of these geothermal resources in a case study in southern Italy, characterized by a widespread abundance of carbonate units up to great depths. The formations present a variety of subsurface temperature gradients which are representative for non-magmatic areas, measured in the frame of oil and gas exploration.

The last geothermal potential assessment in Italy was carried out at the end of the 1980s with the completion of the Inventory of the Italian Geothermal Resources. This involved a joint venture including ENEL, ENI, ENEA and CNR, and published by Cataldi et al. [14]. In the assessment, Italy was divided and ranked in seven categories on the basis of the presence of a regional aquifer of up to 3 km depth and on the temperature range of the fluid. However, this survey failed to clearly identify the carbonate potential reservoirs. Moreover, a quantitative geothermal potential has never been established in Italy, and the few available estimates [[15] and references therein] are based on semi-quantitative assumption.

In this paper we propose a new approach to the geothermal potential assessment through a resource assessment built from a voxel¹ based subsurface representation of rock properties and a comprehensive techno-economic evaluation of prospectivity [16,17]. The resulting procedure, named VIGORTermoGIS, produces geothermal potential maps on the basis of the thermal energy needed and the availability of suitable carbonate reservoirs underground.

This procedure was set up in with the framework of the VIGOR project aimed at assessing the regional geothermal potential in four regions of southern Italy: Apulia, Calabria, Campania and Sicily. The computation was applied to the regional on land geothermal reservoir, thus minor volcanic islands and off-shore areas were not considered.

3. Methodology

The most commonly-used method for geothermal potential assessment relies on volumetric approaches by estimating the thermal energy available in a deep-seated reservoir and the recoverable fraction suitable for the exploitation from technical and/or financial perspectives. The principles of the volume method have been widely discussed and applied by several authors since the 1970s [18–26] above all to assess the geothermal potential in hydrothermal systems. The volume method was subsequently revised and reused in order to compute the geothermal potential for EGS (Enhanced Geothermal Systems) in several countries [27–30, 17, 31–33].

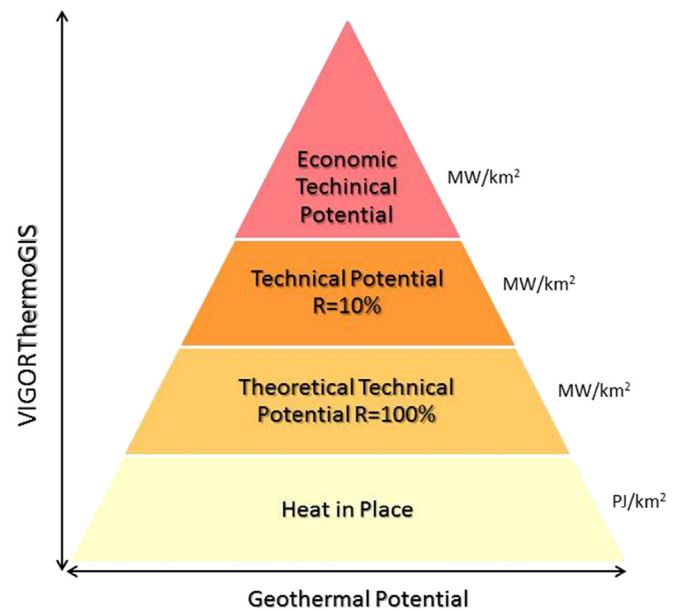


Fig. 1. Progressive geothermal potential filtering, from the Heat in Place to a more realistic Economical Technical Potential.

The geothermal potential assessment in southern Italy was performed by setting up a procedure (VIGORTermoGIS) based on the volume method. The procedure takes into account the practices set up by TNO to assess the prospective areas for geothermal development in the Netherlands (ThermoGIS) [34]. ThermoGIS aimed to evaluate the geothermal potential over several stacked siliciclastic reservoirs. The code was also used within the framework of the GEOELEC project [35] to perform geothermal EGS potential in Europe [36,17]. To address specific features of the geological and geothermal framework in southern Italy, we updated the existing ThermoGIS code. Our assessment focused on the deep geothermal resources, limited to a maximum depth of 5 km below sea level. Such resources are usually hosted in the main regional carbonate units [37]. Below such depth, at the actual drilling cost geothermal exploitation would be not economically feasible (drilling technology is not so limited, and proved up to 10 km).

The VIGORTermoGIS uses a 3D model of the subsurface represented by a voxel with cells (i.e., voxels), with a typical horizontal resolution of 1 km and a vertical resolution of 100 m.

The procedures compute the geothermal potential on the basis of three main components: i) the resource, considering the geometry and the petrophysical properties of the reservoir, ii) the application, which includes in the assessment the specific application technology features and iii) the finances involved, which ensures the energy production estimation taking into account the costs for energy production.

The resource is defined by the geometry of the reservoir, the temperature distribution in the subsurface, the expected rock permeability, and the thermal properties of the fluid-rock system.

VIGORTermoGIS provides a series of geothermal potential maps, such as a heat in place map (H), a technical potential map (TP), and an economic technical potential map (ETPlcoe).

The EPP (electric power production) with binary plant, DH (district heating) and DHC (district heating and cooling) applications were considered in this study. Other typical applications for the direct use of the heat were not taken into account as the regional geothermal reservoir is located at an uneconomical depth.

¹ A Voxel is defined as a regular gridded subsurface 3D model, consisting of brick-shaped hexahedra.

Table 1
Geothermal potential output maps represented as a grid map.

| Potential | Name | Unit |
|-----------|--|--------------------|
| H | Heat in place | PJ/km ² |
| TPtheory | Theoretical technical potential (R = 1) | MW/km ² |
| TPvigor | Technical potential (R = 0.1) | MW/km ² |
| ETPlcoe | Economic technical potential (LCoE < cutoff) | MW/km ² |

To obtain the most realistic geothermal potential for the specific application, VIGORThermoGIS uses gradual filtering, starting from the heat budget in the reservoir (Fig. 1). The filters are based on specific reservoir and application figures and they indicate the heat in place, as well as the theoretical, technical and economic potential [34].

3.1. Heat in place

Firstly the geothermal potential was computed as the heat in place (H), which is the maximum theoretically available heat from

the reservoir. The H value for each cell, H_i, of the 3D grid results from the equation:

$$H_i [PJ/km^2] = V_i * \rho_{rock_i} * C_{p_{rock_i}} * (T_i - T_s) * 10^{-15} \tag{1}$$

where V_i is the volume (m³), ρ_{rock} is the density (kg m⁻³), C_{p_{rock}} is the specific heat (J kg⁻¹ K⁻¹), T_x is the temperature at depth x, and T_s is the surface temperature, according to [20]. The map of H is calculated as the vertical sum of the grid cells divided over the surface area of the grid cells in km², see Table 1.

3.2. Technical potential

Each application is characterized by technical parameters, such as the efficiency of the thermodynamic cycle, the minimum operating temperature (production temperature T_x) and the output temperature (re-injection temperature T_r). At this stage of

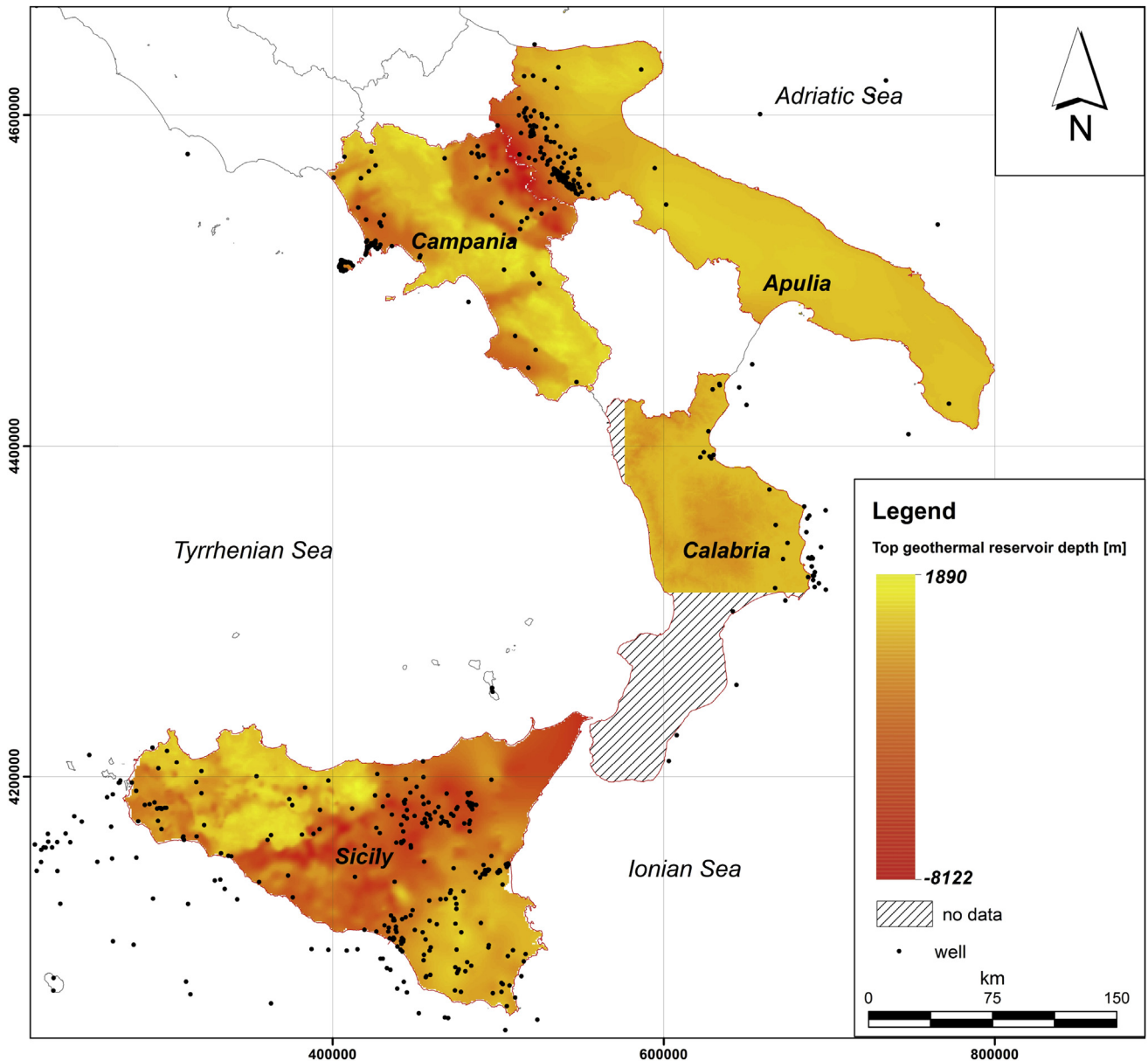


Fig. 2. Top reservoir surface along Campania, Calabria, Apulia and Sicilia.

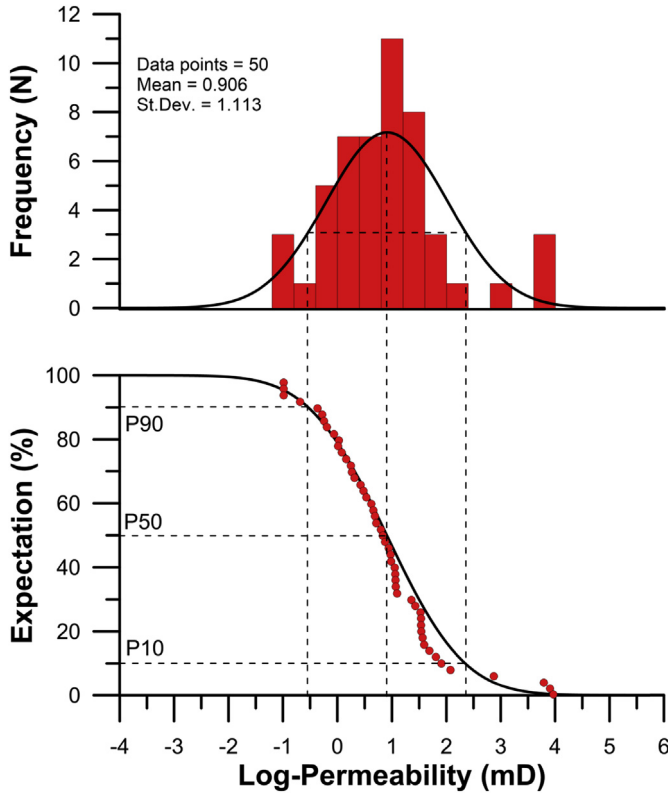


Fig. 3. Log-normal distribution of permeability data.

computation, those voxels that did not meet the minimum required temperature were rejected.

For electricity production, following Beardsmore et al. [29], T_r is:

$$T_r = T_s + 80 \text{ } ^\circ\text{C}$$

where T_r is the base temperature (re-injection temperature) and T_s is the average surface temperature. The base temperature is a key

Table 2

Petrophysical properties of the regional reservoir assigned in the geothermal potential computation (a), technical parameters for the applications assessed, * relative efficiency value (Carnot cycle) (b), and economic technical parameters used to obtain the ETP for power production (c).

| a) Petrophysical parameters | | | | | |
|---|---------------------------|--------------------|------------------------------|-----------------|-----------------------|
| | Calabria | Campania | Apulia | Sicity | |
| Density (kg/m ³) | 2650 | 2650 | 2775 | 2775 | |
| Heat capacity (J/(K kg)) | 900 | 900 | 1040 | 1040 | |
| Average permeability (mD) | 8.5 | 8.5 | 75.8 | 8.3 | |
| Permeability Std. Dev. | 7.6 | 7.6 | 10.2 | 13.5 | |
| b) Technical parameters | | | | | |
| | Electric power production | District heating | District heating and cooling | | |
| Minimum production temperature (°C) | 120 | 80 | 60 | | |
| Re-injection temperature (°C) | 107 | 44 | 33 | | |
| Plant efficiency | 0.6* | 1 | 0.7 | | |
| Recovery factor | 10 and 100% | 10 and 100% | 10 and 100% | | |
| c) Technical-economic parameters for power production ETP | | | | | |
| Well system | COP hydraulic pump | Wells distance (m) | Reservoir net pay (m) | Load hours/year | LCOE threshold (€/MW) |
| doublet | 20 | 1000 | 1000 | 6700 | 200 |

assumption in these estimates and represents the temperature to which can theoretically be reduced through utilization of geothermal heat [29]. In order to conservatively maintain the thermal state of the reservoir, T_r was increased by 10% in the computation.

Eq. (1) thus becomes:

$$H_i \left[\frac{\text{PJ}}{\text{km}^2} \right] = V_i * \rho_{rock} * C_{p_{rock}} * (T_i - T_r) * 10^{-15} \quad (2)$$

The TP (technical potential) returns the producible thermal energy during the mean plant lifespan, here considered as 30 years. The TP depends on the actual recoverable thermal energy from the reservoir. VIGORThermoGIS returns the theoretical TP which considers 100% energy recovery (TP_{theory}) and TP scaled by a recovery factor (R) which denotes the practical efficiency of the thermal exchange between rocks and fluid (TP_{vigor}) in an exploited volume at larger spatial scales, see Table 1. TP is therefore:

$$TP_i \left[\frac{\text{MW}}{\text{km}^2} \right] = \frac{H_i * \eta * R * 10^{15}}{30 \text{ year} * (\text{seconds per year}) * 10^6} = 1.057 * H_i * \eta * R \quad (3)$$

where η is the efficiency [38] expressed as:

$$\eta = \frac{T_i - T_s}{T_i + T_s} * 0.6 \quad (4)$$

with T_i and T_s in Kelvin degrees.

Defining and computing R is key in geothermal potential assessments [20,21,39, 26, 28,29,27,30,36, 31, 32,33]. The value of R depends on, for example, fractured volume of rock, permeability, and rock temperature. R ranges from 0.01 for an EGS (Enhanced Geothermal System) [4] to the theoretical maximum value of 0.5 for a hydrothermal reservoir [36]. Without any direct geothermal production information in the studied areas, the use of a mean value comprised between 0.02 and 0.20 was suggested by Beardsmore [29], thus the average value of 0.1 is used in our work.

The TP maps are calculated as the vertical sum of the grid cells divided over the surface area of the grid cells in km².

3.3. Economic technical potential

The economic technical potential (ETP_{lcoe}) is extracted from the TP_{vigor} (TP with R = 0.1), accepting only those cells of the 3D grid where the Levelized Cost of Energy (LCOE) is less than a given threshold. The LCOE is computed as the ratio of the accumulated discounted cost over the lifetime of the doublet and the accumulated discounted energy [16].

Many financial and technical factors affect the LCOE, such as the drilling, plant operating and maintenance costs. In addition, there is the whole cash flow related to the lifespan of the plant, the inflation rate, interest on loans, taxes, and even a possible feed-in-tariff.

The cash-in flow is strictly related to the performance of the reservoir since its hydraulic transmissivity controls the flow rate (Q) of the geothermal fluid exploited by the well and hence the producible energy. To calculate the flowrate from the transmissivity, it is assumed that the geothermal plant consists of a doublet system, where the production well and the re-injection well are 1000 m from each other, and the flow rate Q is given by Ref. [16]:

$$Q = \Delta p \left(\frac{2\pi k h}{\mu_{inj} \left(\ln \left(\frac{L}{r_w} \right) \right)} + \frac{2\pi k h}{\mu_{prod} \left(\ln \left(\frac{L}{r_w} \right) \right)} \right) \quad (5)$$

Where Δp is the pressure to drive the flow at the reservoir level, which is at maximum limited to 10% of the hydrostatic pressure, k is the permeability, L is the distance between the injector and producer, r_w is the well radius, μ is the viscosity which differs in terms of the injection and production temperature, and h is the thickness of the reservoir [16]. In the calculation, Δp is limited as well by constraining the maximum coefficient of performance (COP), which is defined as the ratio of heat produced and the pump energy required to drive the pumps of the doublet. h may be larger than the cell size, in which case Q is divided over multiple cells, and k is based on the average of k in the cells.

In order to compute the LCoE, the energy available in each volumetric cell is derived as:

$$\text{Energy [MW]} = Q * \rho_{\text{water}} * C_{p\text{water}} * (T_x - T_r) * \eta * 10^{-6} \quad (6)$$

where Q is assigned to each reservoir voxel on the basis of the expected transmissivity for a certain cumulative probability computed by the Monte Carlo Simulation, ρ_{water} is the fluid density (kg m^{-3}), $C_{p\text{water}}$ is the fluid specific heat ($\text{J kg}^{-1} \text{K}^{-1}$), T_x is the temperature at depth x , and T_r is the re-injection temperature. In ETPlcoe denotes the 50% expectation in the cumulative probability. It should be noted that transmissivity is considered key in terms of uncertainty, as typically transmissivity is an order of magnitude more uncertain and its effect is significantly more pronounced in LCoE than the uncertainty effect in any of the other properties (see, for example, [16]).

The map of ETClcoe is calculated as the vertical sum of only those grid cells of TPvigor in which the LCoE computed value is lower than a given threshold divided over the surface area of the grid cells in km^2 , see Table 1.

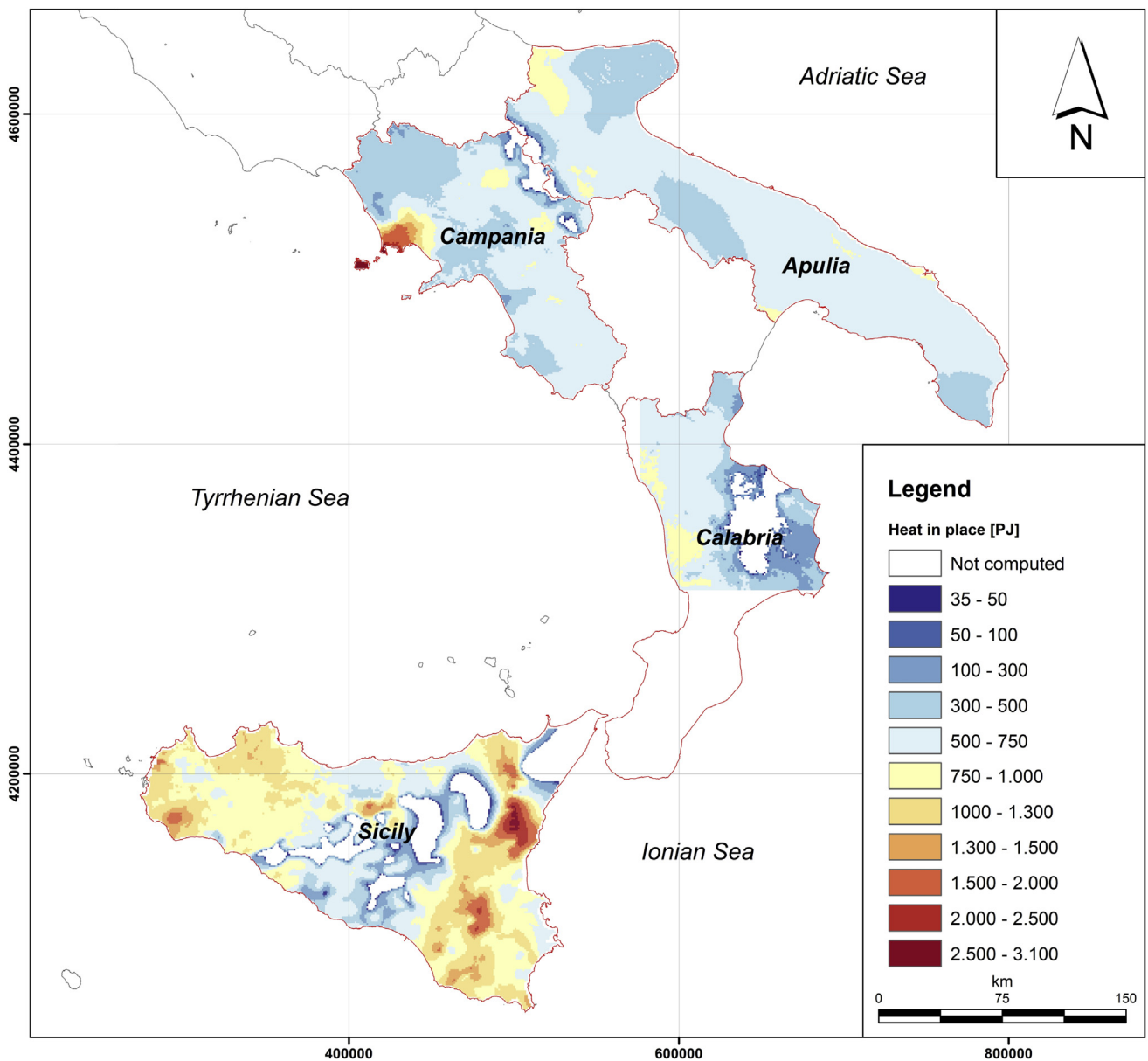


Fig. 4. Heat in place (H) map for Sicily, Apulia, Campania and Calabria.

4. Input data for geothermal potential computation of southern Italy

4.1. Reservoir geometry

The regional scale geothermal reservoir is located within the Meso-Cenozoic carbonates and could host low (<90 °C) to medium (<150 °C) geothermal resources [40,41]. In order to assess the geothermal potential up to a 5 km depth b.s.l., a 3D geological modelling for Calabria, Campania, Apulia and Sicily was required. For each region, we performed the 3D reconstruction of the top of the regional geothermal reservoir by integrating public and

confidential geological, geophysical and deep exploratory well data, as described by Montanari [37] for Sicily.

The 3D simplified geological model is built up by starting from the top: i) siliciclastic basinal units of very different ages representing the impermeable cap-rock and ii) thick and widespread Meso-Cenozoic carbonates units constituting the regional geothermal reservoir.

In southern Calabria, where crystalline units widely crop out and the carbonates units are assumed to be absent at depth (i.e., at least up to the investigated 5 km bsl), a 3D reconstruction of the geothermal reservoir was not possible due to the complete absence of data. Consequently we were unable to compute the geothermal potential.

4.2. Thermal model

In order to constrain the temperature distribution, we selected 564 deep exploratory wells providing exhaustive temperature measurements and litho-stratigraphic information (Fig. 2). [42,43,44] or kindly provided by ENI S.p.A.

Bottom hole temperatures (BHTs) measured in the hydrocarbon exploration wells were the main source of information for constructing a subsurface thermal model. The cooling effect of the circulating drilling mud was evaluated to make appropriate corrections to the raw data, thus leading to an adequate estimation of the real formation temperature.

We evaluated the average linear geothermal gradients site-by-site by litho-thermal units grouped by similarities in lithology and thermo-hydraulic properties, according to the methodology proposed in Trumpy et al. [45]. The selected wells were sufficiently deep that the lower section of the temperature-depth profile could be used for a suitable determination of the geothermal gradient, which was presumably free of topographic and paleo-climatic effects. The temperature data highlighted locally high geothermal gradients in the sedimentary cover units and very low gradients in the deep-seated carbonate ones. The lower values observed in the reservoir units could be due to the higher thermal conductivity of carbonate rocks compared to the clay-rich ones in the cover units. However, we argue that locally such a vertical change cannot be ascribed to thermal conductivity variations within the litho-stratigraphic sequence. The deep groundwater flow can affect the actual temperature distribution and where the hot geothermal fluids rise within the reservoir can lead to positive thermal anomalies in the cap-rock units.

To study the temperature distribution at depth we adopted a combined geostatistical geothermal gradient interpolation [46] and downward temperature extrapolation method supported by geological knowledge (see Ref. [45] for details). The temperature field was derived by a combination of the annual mean surface temperatures [47] and regionally varying geothermal gradients in relationship with the cover-reservoir boundary depth model. We computed the subsurface temperature (i.e., the 3D thermal voxel) through a 3D mesh grid of 1000 × 1000 × 100 m³ along the latitude, longitude and depth, respectively. Due to the scattered spatial distribution of the boreholes and the low vertical resolution of the temperature data, a large degree of extrapolation at the first stage of the geothermal resource assessment was necessary. We took care to apply the thermal gradient within the same litho-thermal unit, highlighting the role of the thermal gradient contrast existing at the cover-reservoir boundary, as well as the effect of water circulation inside the permeable reservoir.

Table 3

Computed thermal energy (H) stored in the deep-seated carbonate reservoir units (a), technical potential (TP) for the direct uses and electrical power generation (b), and the economic technical potential for electrical power generation (c). The table reports the minimum, maximum and the average values of the H, TP and ETP by square kilometre (standard deviation in brackets) and the Total H, TP and ETP. S_{tot} is the total regional surface, S_{res} is the percentage of the regional surface in which carbonate reservoir units are present in the first 5 km depth, S_{TP} is the percentage of the regional surface below which the minimum thermal conditions occur in the first 5 km depth.

| a) Heat in place | | | | | | |
|------------------|------------------------------|---------------|-------------------------|-------|------------|--------------|
| Region | S_{tot} (km ²) | S_{res} (%) | H (PJ/km ²) | | | Total H (PJ) |
| | | | min | max | av (StDev) | |
| Calabria | 15,082 | 52 | 25 | 863 | 511 (214) | 3,994,728 |
| Campania | 13,595 | 94 | 32 | 3,370 | 559 (253) | 7,176,416 |
| Apulia | 19,345 | 95 | 42 | 1,055 | 584 (110) | 10,737,364 |
| Sicily | 25,711 | 84 | 30 | 2,857 | 860 (380) | 18,499,005 |

| b) Technical potential (R = 10% – Utilization = 30 years) | | | | | |
|---|---|------|------|-------------|------------------------------|
| Region | DH | | | | |
| | TP (MW _{th} /km ²) | | | | Total TP (MW _{th}) |
| | S_{TP} (%) | min | max | av (StDev) | |
| Calabria | 52 | 2.01 | 69.6 | 36.4 (15.1) | 284,777 |
| Campania | 83 | 0.91 | 338 | 30.5 (31.0) | 344,722 |
| Apulia | 68 | 1.20 | 73.1 | 17.4 (12.7) | 230,458 |
| Sicily | 83 | 1.20 | 278 | 57.5 (36.0) | 1,222,451 |

| DHC | | | | | |
|----------|---|------|------|-------------|------------------------------|
| Region | TP (MW _{th} /km ²) | | | | Total TP (MW _{th}) |
| | S_{TP} (%) | min | max | av (StDev) | |
| | Calabria | 52 | 1.60 | 54.6 | 31.0 (12.6) |
| Campania | 94 | 0.48 | 242 | 27.6 (20.5) | 354,350 |
| Apulia | 95 | 2.68 | 63.5 | 21.6 (9.6) | 397,661 |
| Sicily | 84 | 1.81 | 202 | 49.9 (30.0) | 1,073,720 |

| EPP | | | | | |
|----------|--|------|------|------------|-----------------------------|
| Region | TP (MW _e /km ²) | | | | Total TP (MW _e) |
| | S_{TP} (%) | min | max | av (StDev) | |
| | Calabria | 49 | 0.05 | 4.1 | 1.0 (0.8) |
| Campania | 24 | 0.05 | 88.1 | 5.2 (11.0) | 16,814 |
| Apulia | 5 | 0.07 | 3.8 | 1.0 (0.6) | 1,017 |
| Sicily | 61 | 0.07 | 56.6 | 3.3 (5.2) | 52,190 |

| c) Economic-technical potential (P50 and LCoE < 200 €/MW _e) | | | | | |
|---|---|------|------|--------------|------------------------------|
| Region | EPP | | | | Total ETP (MW _e) |
| | ETP (MW _e /km ²) | | | | |
| | S_{TP} (%) | min | max | av (StDev) | |
| Calabria | – | – | – | – | – |
| Campania | 24 | 0.57 | 88.1 | 24.4 (16.96) | 13,133 |
| Apulia | 5 | 0.39 | 3.63 | 1.47 (1.03) | 22 |
| Sicily | 11.5 | 0.21 | 56.6 | 9.28 (9.06) | 27,476 |

4.3. Permeability assessment

Permeability is the most important petrophysical reservoir parameter as it directly determines the productivity of the well and thus the rate at which the thermal energy can be extracted from the geothermal reservoir. On the other hand, this is also the most difficult parameter to calculate, as it is usually characterized by an extremely high spatial variability. We estimated the permeability of the carbonate formations by interpreting the DSTs (drill-stem tests) from several hydrocarbon exploration wells. The average depth of the tested intervals spans from about 800 m to over 4500 m, with a typical thickness (*a*) of about 50 m.

Since a complete set of build-up pressure data recorded as a function of time is rarely available, we processed the pressure data assuming the following ideal conditions [48,49,50]: i) pseudo-steady-state flow regime, ii) homogeneous and infinite reservoir, and iii) single-phase radial flow. The transmissivity of the reservoir

was described in terms of the productivity index, based on the flow rate and pressure drawdown data collected in the DST reports. We calculate the permeability by assuming the productive vertical thickness equals the whole tested interval. Water and oil viscosity are assigned according to [51] and from the laboratory analysis reports, respectively.

The results provided values for the real level of permeability, under reservoir conditions, referring to a larger rock volume than the laboratory core analysis. The computed permeabilities are widely scattered ranging from $1.0 \cdot 10^{-15} \text{ m}^2$ to $8.0 \cdot 10^{-13} \text{ m}^2$.

Since the permeability data do not display a clear relationship with depth, we treated the permeability of the regional reservoir as a spatially random variable and hence we described the reservoir productivity for a larger than tested average interval by applying Monte Carlo procedures.

This approach provided an excellent methodology to predict production profiles with a wide variety of reservoir

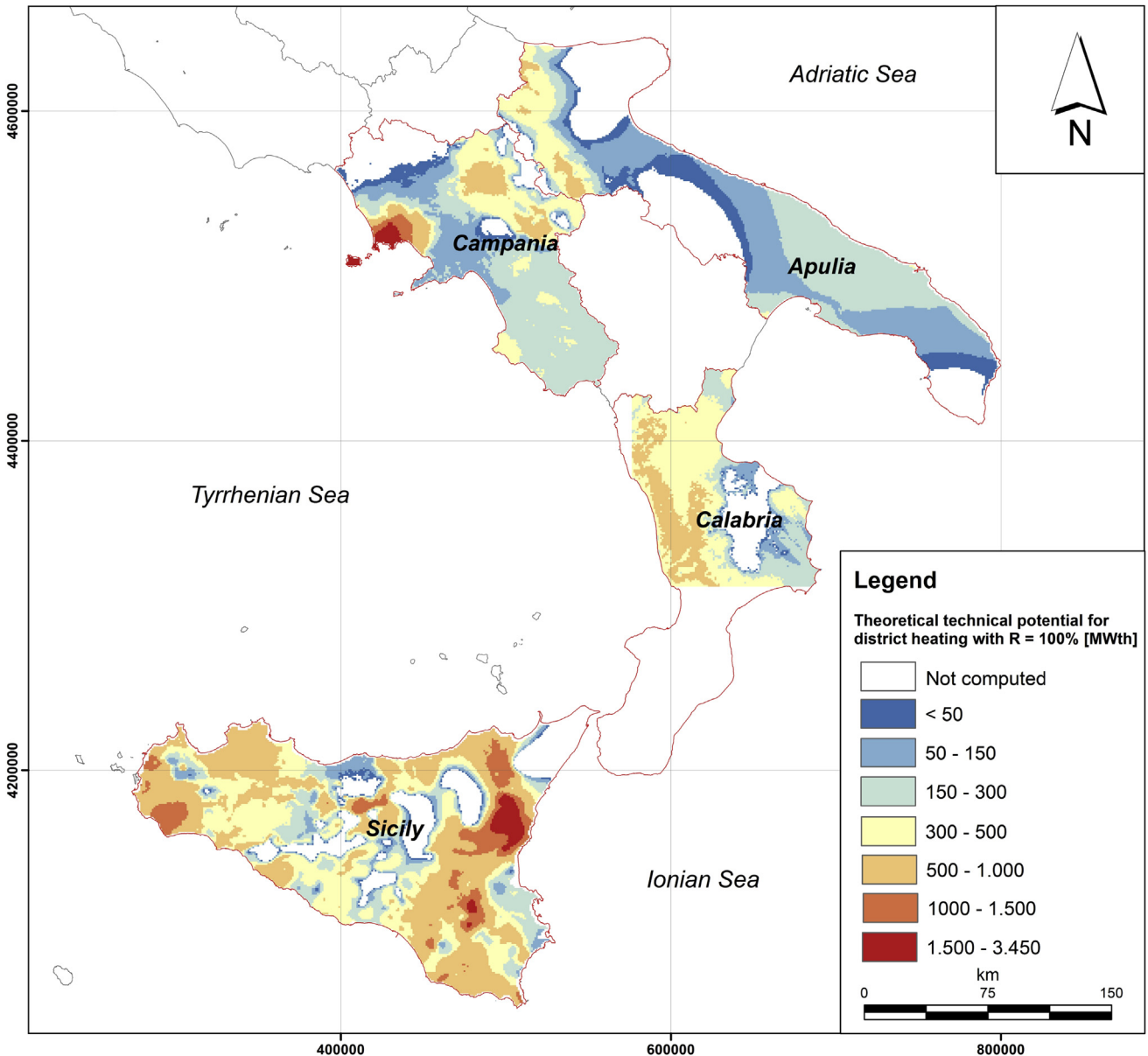


Fig. 5. Theoretical technical potential for district heating with R = 100%, TPtheory.

characteristics and production conditions. The average permeability for an interval of up to 50 m is assumed as log normal and depends on two parameters: the average value (mathematical estimate) and the range of deviations from the average value (dispersion). The dispersion identifies the level of the heterogeneity of the reservoir. Fig. 3 shows an example of a permeability probability function. For productive intervals with a thickness (h) larger than 50 m, the average permeability is obtained as the average of the N repeated Monte Carlo prediction values, where $N = h/a$.

5. Results and discussion

The following tables and maps were obtained by using the following as input data for VIGORThermoGIS: i) the grid surface of

the depth of the regional deep-seated geothermal reservoir; ii) the 3D thermal voxel, described in Subsection 4.2; and iii) a set of physical properties related to the fluid-rock system, technical and economic features of the plant, shown in Table 2.

The H in the four regions of southern Italy was determined by VIGORThermoGIS by applying Eq. (1), shown in Fig. 4. Table 3a summarizes by region the H stored in the carbonate units, which act as regional reservoirs, in the first 5 km depth. In the studied regions the overall H (obtained by summarizing the H value from each cell) results in the order of $4 \cdot 10^7$ PJ for a total area of $60,500 \text{ km}^2$.

The technical potential with an R factor of 1 and 0.1 (100% energy recovery and 10% energy recovery) obtained with Eq. (3) are presented for district heating in Figs. 5 and 6, district heating and cooling in Figs. 7 and 8, and electric power production in Figs. 9 and 10 respectively.

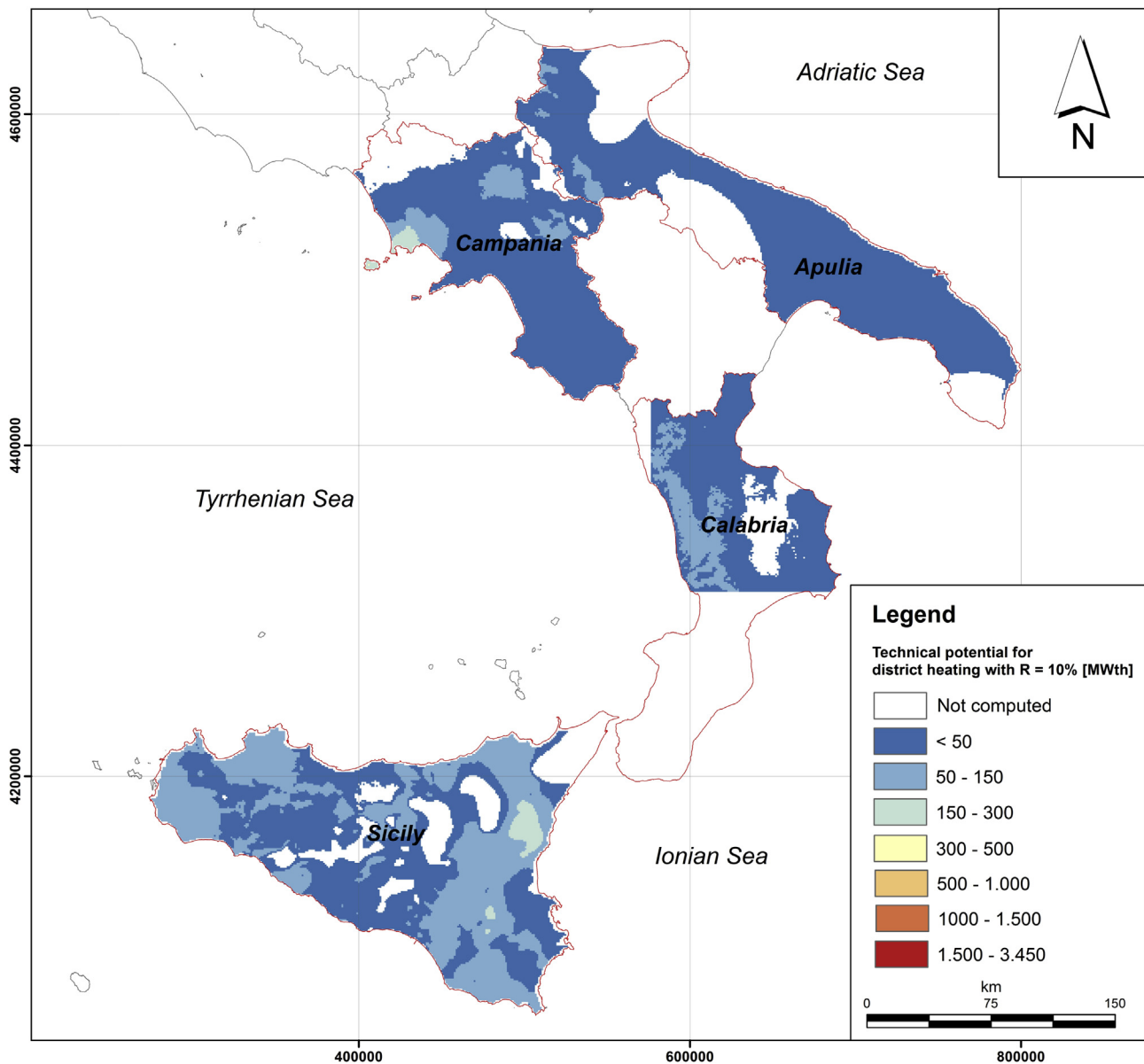


Fig. 6. Technical potential for district heating, with $R = 10\%$, TPtheory.

The total technical potential (TP_{vigor}, R = 0.1) in the four regions is evaluated as 2082 GW_{th} for the District Heating (DH), 2168 GW_{th} for the District Heating and Cooling (DHC) and 77 GW_e for the EPP (Electrical Power Production), see Table 3b for details.

The ETP (economic technical potential) for DH and DHC applications was not computed due to the difficulty in estimating important parameters such as plant costs and the distribution network costs closely tied to the fluid characteristics and the dimension of the area to be served. We report the computation of the ETP for power production for which the economic values can be constrained by site-independent experience.

Fig. 11 represents the corresponding economic technical potential map for power production, where the producible MW_e were computed only in the voxel elements where the LCoE, referring to a value of hydraulic permeability expected with a probability of 50%, is below the given threshold of 200 €/MW_e [17,52].

5.1. From economic technical potential to the IEC (installable electrical capacity)

The geothermal potential map has the advantage to show clearly the areas having the best chances for geothermal development. The amount of energy production that could realistically be installed, however, cannot be simply the sum of all the grid cell values, because it is impossible to install a plant in every km².

Currently, there is no well-defined and unique methodology in the literature that determines the installable electrical power from the geothermal potential.

In this work we have proposed a VIGORThermoGIS post-processing analysis of the ETP map for power production in order to estimate which part of the geothermal potential could be used realistically by geothermal binary plants at the regional scale. We called this geothermal potential, the IEC (installable electrical capacity).

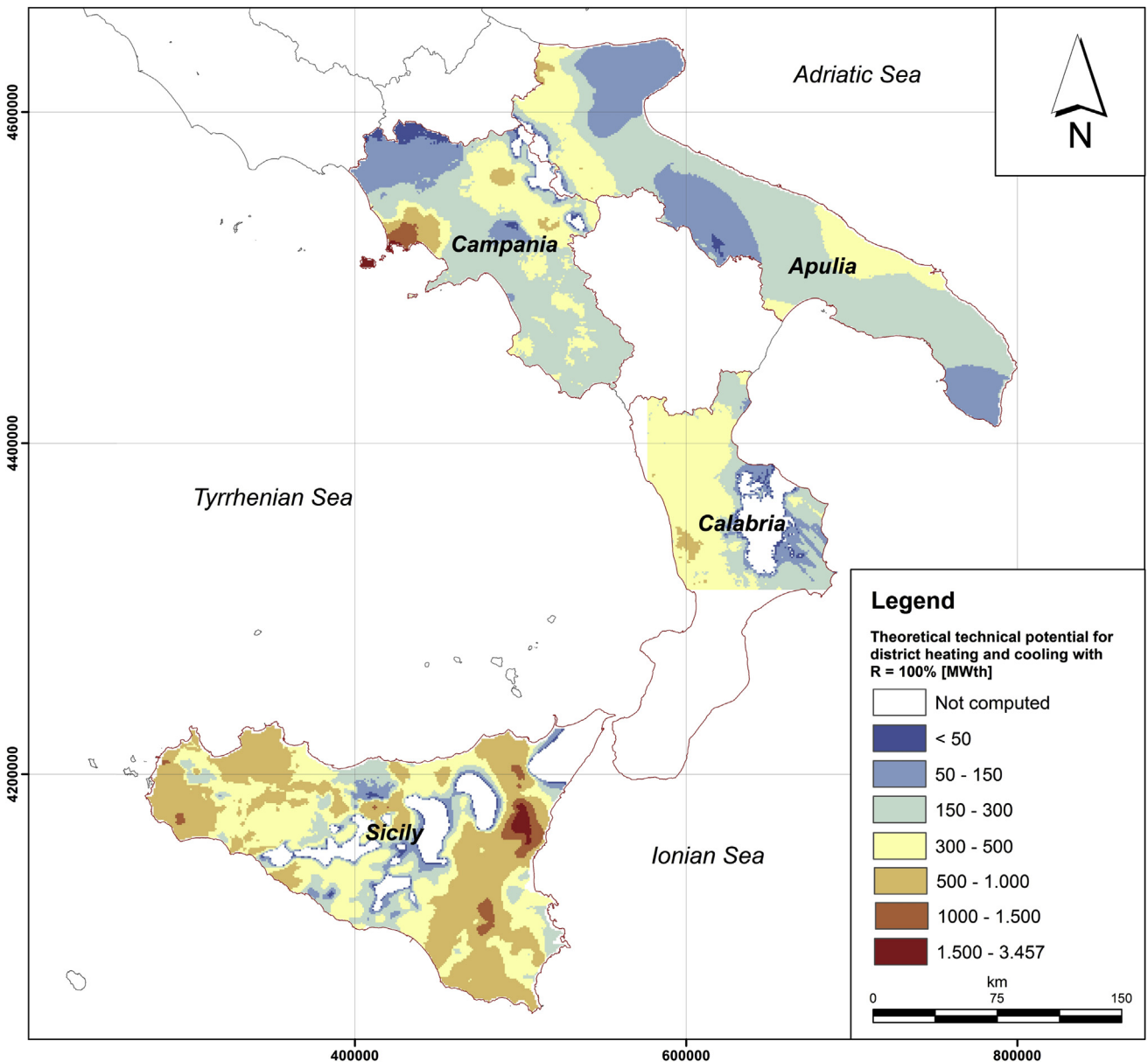


Fig. 7. Theoretical technical potential for district heating and cooling, with R = 100%, TP_{theory}.

The post-processing analysis consists in applying a series of further filters on the ETP map which take into consideration environmental and technical issues.

Firstly we recomputed the ETP map (ETP_{lcoe}) assuming the carbonate units are productive in only one voxel (i.e., a net pay thickness of 100 m in our case) as a maximum reservoir. This takes an average value of energy, and makes the estimation more realistic.

Secondly from the map obtained with the previous filter we discarded areas with an acclivity higher than 15%, which enabled us to consider only the areas with a morphology suitable for power plant installation.

We then considered 25% of the value of each cell of the map as we hypothesized that an area of 4 km² (cell 2 km × 2 km) was needed to install the plant and the well doublet. This consideration is related to the optimized geometrical configuration of the doublet system used in this study to avoid thermal interference inside each

cell and with the adjacent ones. As the production and the re-injection well bottoms are separated by 1 km, in order to install the plant respecting this constraint, a square cell of 2 km × 2 km was needed made up of four pixels (1 km × 1 km).

The regional scale ETP* (* denotes the post-processed ETP) was obtained as the sum of the pixel values in the post-processed computed map, see Table 4. Eventually the total amount of ETP* per region was then further reduced by a scale factor *f*, which enables the IEC to be estimated heuristically. The scale factor is the ratio between the IC (installed capacity) in MWe and the assessed geothermal potential. We estimate *f* from the Wabuska geothermal field in Nevada (US) which is comparable with the low to medium hydrothermal systems in southern Italy [42,53]. The IC for Wabuska was retrieved from the Global Geothermal Energy Database [54], whilst the TP was obtained from Ref. [55]. Consequently the *f* factor for Wabuska was 0.14, and thus Table 4 reports the final regional installable electrical capacity values.

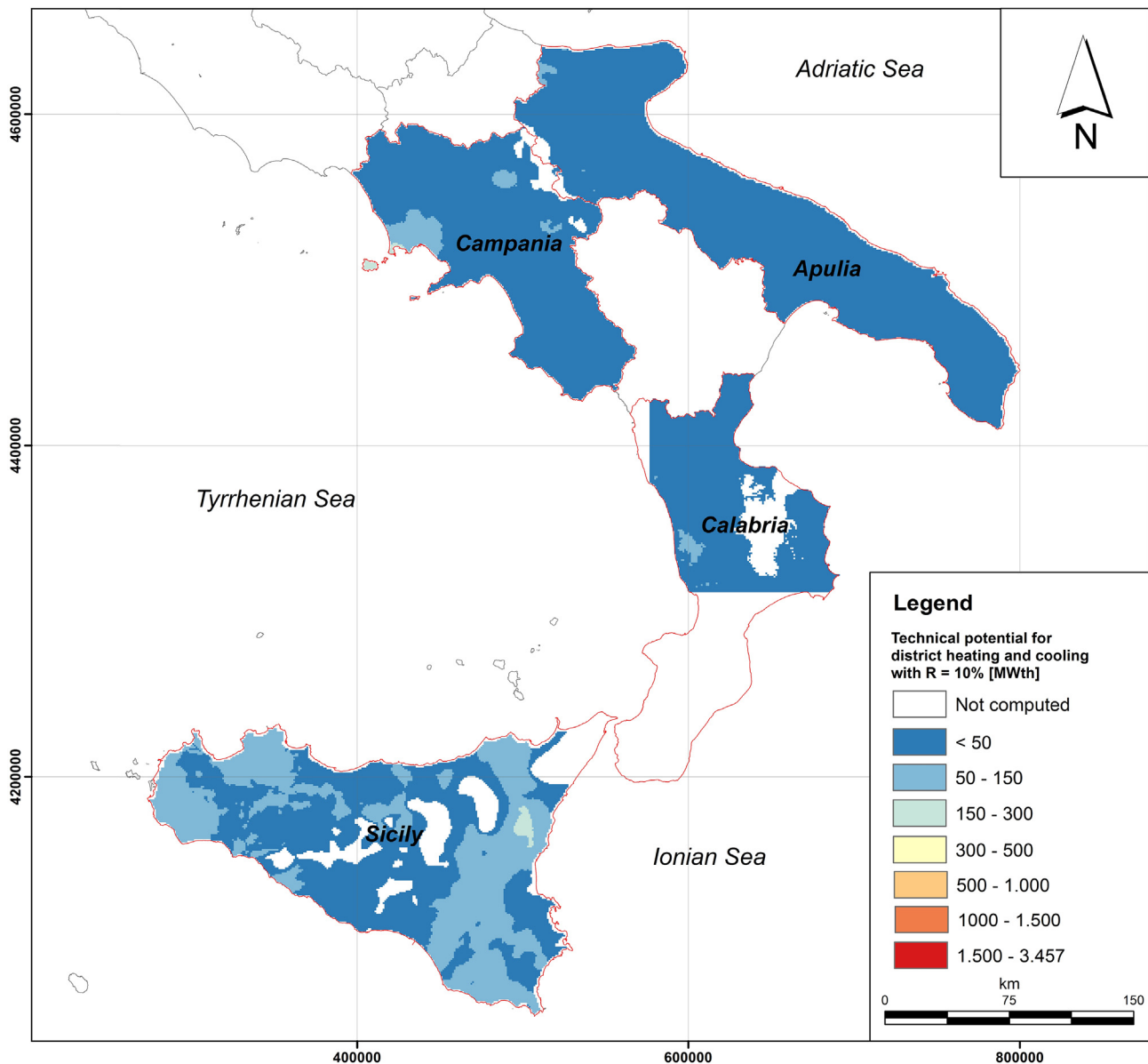


Fig. 8. Technical potential for district heating and cooling, with R = 10%, TP_{vigor}.

5.2. Electricity production

The estimated electricity production at the regional scale is reported in Table 5. The electricity production is obtained as the product of the Total IEC (corresponding to the installable electrical capacity) and the annual load hours of the plant. The load hours are about 95% of the 8760 h per year (the remaining 5% is attributable to the ordinary and extraordinary stops for maintenance) with an employment of about 80% of the installed capacity [15]. These two factors lead to an annual load factor of the plant of 76%, corresponding to an effective load hour of 6700 h/yr.

The electricity produced from geothermal resources strongly supports the reduction in both fossil fuel consumption (oil, gas and coal) and carbon dioxide (CO₂) emissions into the atmosphere. The benefits of energy production from geothermal power plants in terms of saved fossil fuel and avoided CO₂ emissions per year are reported in Table 5. The amount of saved fossil fuel is expressed in

TOE/year [APS website]. Complying with the European Agency for the Cooperation of Energy Regulators, the Italian Regulatory Authority for Electricity Gas and Water set the conversion factor from kWh to TOE in $0.187 \cdot 10^{-3}$ TOE/kWh. Concerning the evaluation of the avoided CO₂, we based our calculation on the average values [15] of 890 gCO₂/kWh, 600 gCO₂/kWh and 950 gCO₂/kWh for oil, gas and coal thermal plants, respectively.

6. Conclusions

We have described a new approach for assessing the geothermal potential at the regional scale along with the results carried out in four regions of southern Italy: Apulia, Calabria, Campania, and Sicily. A heat in place map, theoretical technical potential map, technical potential map for EPP, DH and DHC and economic technical potential map for EPP were all created.

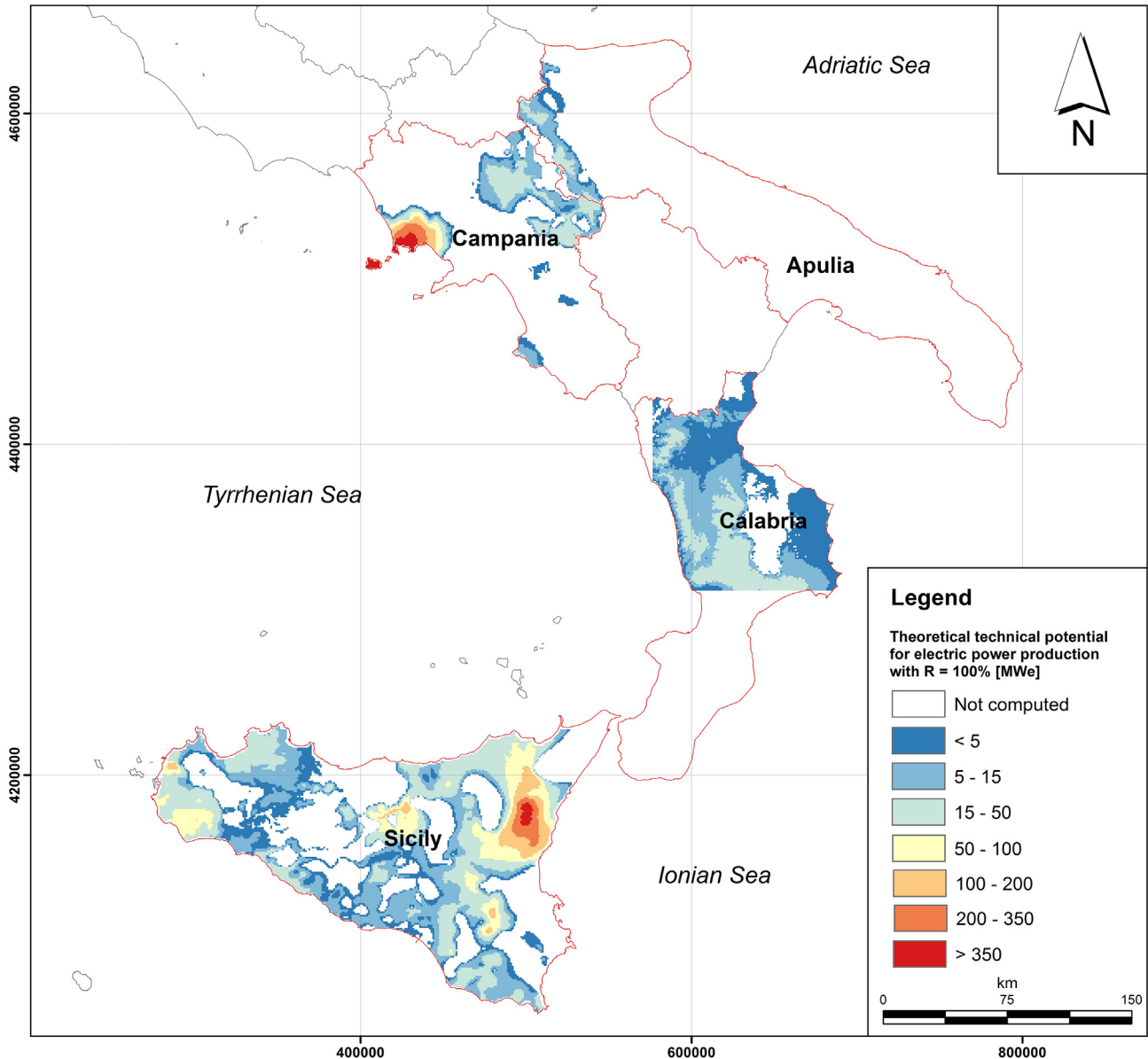


Fig. 9. Theoretical technical potential for electric power production, with R = 100%, TPvigor.

This paper highlights that, unlike what was previously thought, regional mapping of deep regional reservoirs, temperature, petrophysical parameters and flow properties based mainly on hydrocarbon industry data, can provide a major resource base of geothermal energy for direct heat and power production.

Moreover our estimations highlight a total amount of thermal energy available up to 5 km depth in the order of $4 \cdot 10^7$ PJ for the studied areas. This energy guarantees a technical potential of 2082 GW_{th} , 2168 GW_{th} or 77 GW_{e} for district heating, district heating and cooling and electrical power production respectively assuming a life time of 30 years and a recovery factor of 10%. We compute afterward a more realistic economic technical potential, which takes into account financial parameters as well as the uncertainty of the reservoir permeability. For the studied area 551 MW_{e} can be obtained for electric power production.

Eventually, on the basis of reservoir thickness considerations, environmental aspects, doublet system design requirements and

the comparison with similar geothermal areas in production we obtained the total amount of electrical MW installable of 77 MW_{e} . The estimation of the total producible energy, in about 516 $\text{GW}_{\text{e}}/\text{yr}$, allows us to evaluate the total fossil fuel saving of 97 kTOE/yr. Moreover the avoided CO_2 emissions in the atmosphere are expected to be 459 kton/yr, 309 kton/yr and 490 kton/yr for oil, gas and coal, respectively.

The maps obtained in this work represent important tools for all geothermal stakeholders: i) decision makers can use them to establish new policies aimed at fostering geothermal energy, ii) investors can establish where the most promising locations for geothermal exploitation are and calculate the amount of energy available for a specific application.

In the light of this view, the produced maps could represent a key element to propel the process according to which renewable energies, and in particular geothermal energy, can boost the emissions reduction in the region, proposing sites and proper technologies for a more rational planning of energy policies,

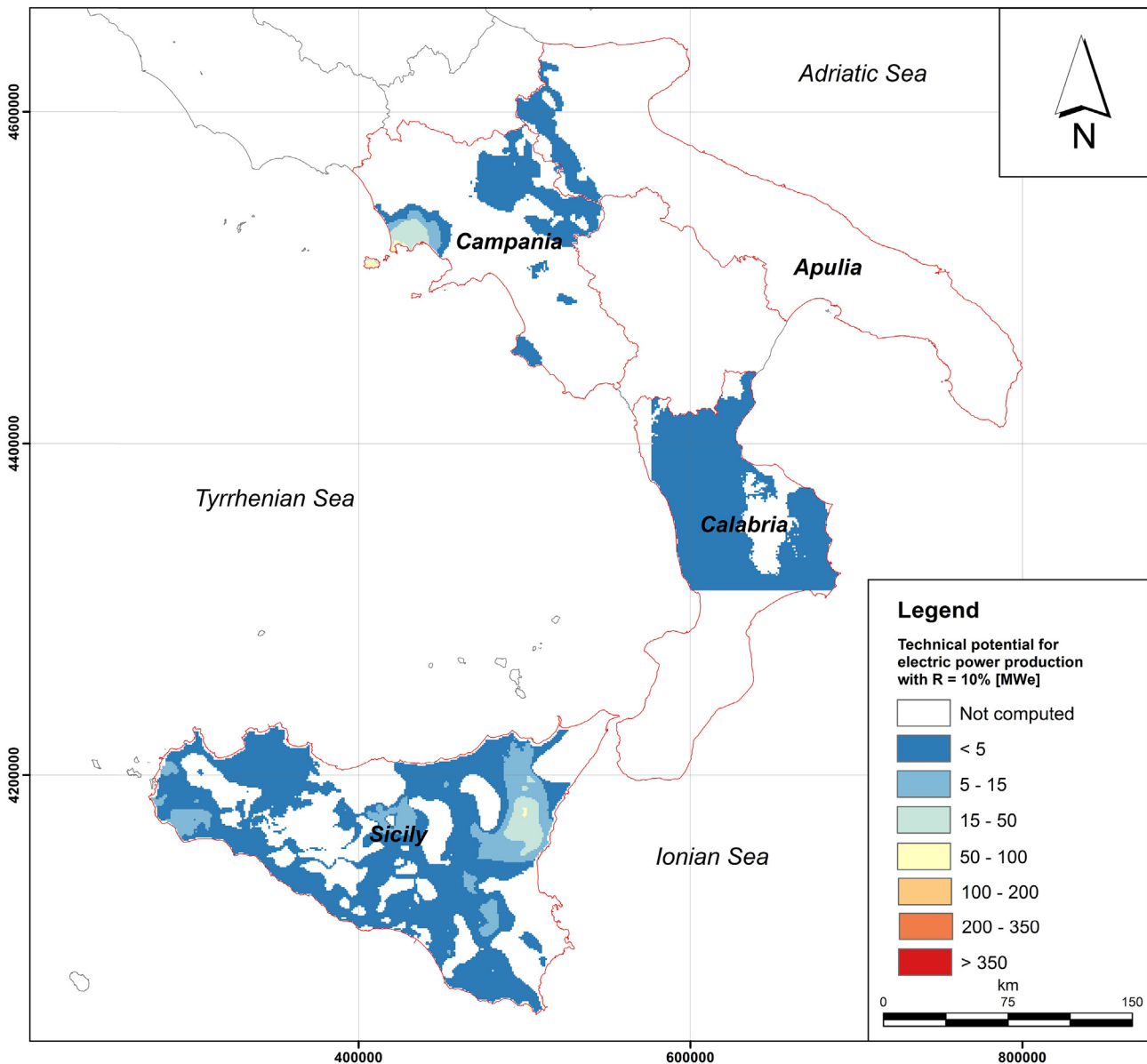


Fig. 10. Technical potential for electric power production, with R = 10%, TPvigor.

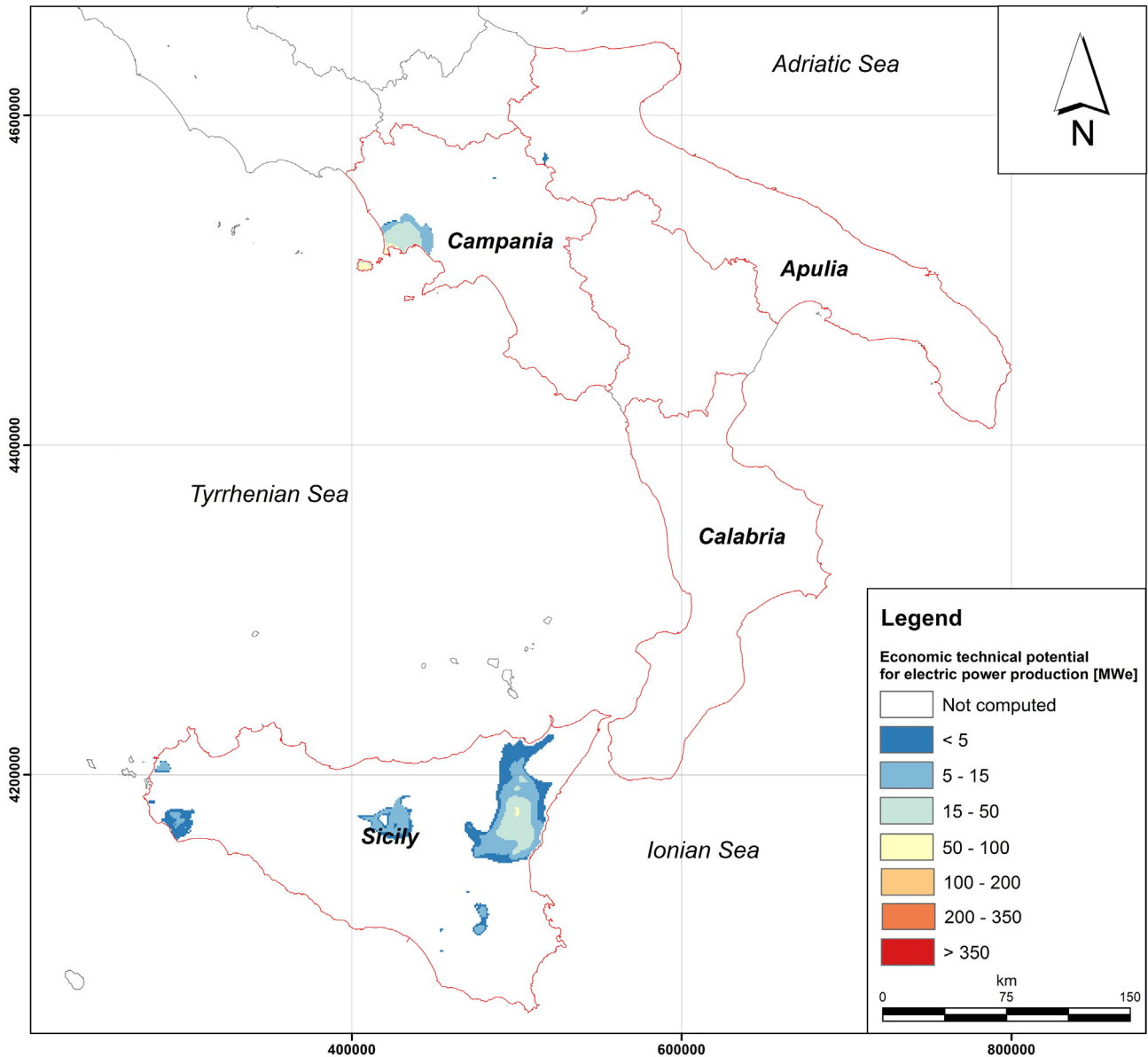


Fig. 11. Economic technical potential for electric power production, ETPlcoe.

according to the geothermal potential assessed in four regions of southern Italy.

The proposed approach is easily reusable not only in the same regions when new and more accurate data are available, but also in

other potential areas where deep-seated carbonate units but in general each kind of regional scale reservoirs were explored in the past providing subsurface data useful again for hydrothermal purpose.

Table 4

The post processed economic technical potential (ETP*) for the EPG application. The minimum, maximum and average (standard deviation in brackets) pixel values are reported. S_{ETP_LCoE} is the regional territory percentage in which there are favourable economic-technical conditions exist. The Total ETP* reports the sum of the pixel values, and Total IEC highlights the MWe obtained with the assessment explained in Subection 5.1.

| Economic-technical potential* (*post-processed) | | | | | | |
|---|-----------------------------|------|------|-------------|------------------|-----------------|
| Region | EPP | | | | Total ETP* (MWe) | Total IEC (MWe) |
| | ETP* (MWe/km ²) | | | | | |
| | S_{ETP_LCoE} (%) | min | max | av (StDev) | | |
| Calabria | — | — | — | — | — | — |
| Campania | 3.8 | 0.05 | 0.87 | 0.3 (0.2) | 157 | 22 |
| Apulia | 0.07 | 0.09 | 0.14 | 0.11 (0.01) | 1.6 | 0.22 |
| Sicily | 10.2 | 0.05 | 0.76 | 0.15 (0.06) | 392 | 55 |

Table 5
Annual electricity production from geothermal resource, fossil fuel savings (in 10³ Tons of Oil Equivalent) and avoided emissions of carbon dioxide (10³ tons of CO₂) as a function of different fossil fuels.

| Region | Regional electricity production | | | | | |
|----------|---------------------------------|--|---------|---------------------------|------|-----|
| | Production | | Saving | | | |
| | Power (MW _e) | Electrical energy (GW _e h/yr) | kTOE/yr | CO ₂ (kton/yr) | | |
| | | | Oil | Gas | Coal | |
| Calabria | 0 | 0 | 0 | 0 | 0 | 0 |
| Campania | 22 | 147 | 28 | 131 | 88 | 140 |
| Apulia | 0.22 | 0.1 | 0.02 | 0.1 | 0.1 | 0.1 |
| Sicily | 55 | 369 | 69 | 328 | 221 | 350 |

Acknowledgements

The present activity was performed within the framework of the VIGOR Project, aimed at assessing the geothermal potential and exploring geothermal resources of four regions in southern Italy. VIGOR is part of the activities of the Interregional Programme (POI) “Renewable Energies and Energy Savings FESR 2007-2013 – Axes I Activity line 1.4 “Experimental Actions in Geothermal Energy”. The authors acknowledge in particular the Managing Authority of POI, Dr. Piezzo of MiSE-DG-MEREEEN (Directorate General for Nuclear Energy, Renewable Energy and Energy Efficiency of the Ministry for Economic Development), Dr. Brugnoli, Director of CNR-DTA (National Research Council of Italy, Department of Sciences of the Earth System and Environmental Technologies) and all the colleagues working in the VIGOR Project for the definition of underground 3D models, referenced in Ref. [41].

References

- [1] UNFCCC website. United Nation Framework Convention on Climate Change, URL: http://unfccc.int/kyoto_protocol/item/2830.php [Last access 27.10.14].
- [2] Edenhofer O, Pichs-Madruga R, Sokona Y, Seyboth K, Matschoss P, Kadner S, et al., editors. IPCC. Cambridge, United Kingdom and New York, NY, USA: Cambridge University Press; 2011. p. 1075. Available from Cambridge University Press, The Edinburgh Building Shaftesbury Road, Cambridge CB2 2RU England.
- [3] Bertani R. Geothermal power generation in the world 2010-2015 update report. In: *Proceedings world geothermal congress 2015*. Melbourne, Australia; 19-25 April 2015.
- [4] Lund JW, Boyd T. Direct utilization of geothermal energy 2015 worldwide review. In: *Proceedings world geothermal congress; 2015*.
- [5] IEA (International Energy Agency). Technology roadmap, geothermal heat and power. IEA Publication; 2011. Available online at: http://www.iea.org/publications/freepublications/publication/Geothermal_Roadmap.pdf [Last access 15/03/2015].
- [6] Kramers L, Van Wees JD, Pluymaekers MPD, Kromius A, Boxem T. Direct heat resource assessment and subsurface information systems for geothermal aquifers; the Dutch perspective. *Neth J Geosci* 2012;91(4):637–49.
- [7] Minissale A, Duchi V. Geothermometry on fluids circulating in a carbonate reservoir in north-central Italy. *J Volcanol Geotherm Res* 1988;35:237–52.
- [8] Molli G, Doveri M, Manzella A, Bonini L, Botti F, Menichini M, et al. Surface-subsurface structural architecture and groundwater flow of the Equi Terme hydrothermal area, northern Tuscany Italy. *Ital J Geosci (Boll Soc Geol It)* 2015;134(3):442–57. <http://dx.doi.org/10.3301/IJG.2014.25>. 12 figs.
- [9] Moek IS, Uhlig S, Loske B, Jentsch A, Ferreiro Mahlmann R, Hild S. Fossil multiphase Normal faults -prime targets for geothermal drilling in the Bavarian Molasse Basin?. In: *Proceedings world geothermal congress; 2015*.
- [10] GeoMol project. Available online at: <http://www.geomol.eu/home/index.html> [Last access 01.12.15].
- [11] Traunreut Geothermal project. Available online at: <http://www.angers-soehne.com/?p=4843&lang=en> [Last access 01.12.15].
- [12] Taufkirchen Geothermal project. Available online at: <http://www.mannvit.com/projects/taufkirchen-kalina-geothermal-power-plant/> [Last access 01/12/2015].
- [13] Unterhaching Geothermal project. Available online at: https://www.geothermie-unterhaching.de/cms/geothermie/web.nsf/id/pa_home.html [Last access 01.12.15].
- [14] Cataldi R, Mongelli F, Squarci P, Taffi L, Zito G, Calore C. Geothermal ranking of Italian territory. *Geothermics* 1995;24(1):115–29.
- [15] Buonassorte G, Cataldi R, Franci T, Grassi W, Manzella A, Mecchieri M, et al. Previsioni di crescita della geotermia in Italia fino al 2030 – Per un Nuovo Manifesto della Geotermia Italiana. 2011. p. 108. Ed. Pacini.
- [16] Van Wees JD, Kromius A, Van Putten M, Pluymaekers MPD, Mijnlief HF, Van Hooff P, et al. Geothermal aquifer performance assessment for direct heat production – methodology and application to Rotliegend aquifers. *Neth J Geosciences Geol en Mijnbouw* 2012;91(4):651–65.
- [17] Limberger J, Calcagno P, Manzella A, Trumphy E, Boxem T, Pluymaekers MPD, et al. Assessing the prospective resource base for enhanced geothermal systems in Europe. *Geoth Energy Sci* 2014;2:55–71. <http://dx.doi.org/10.5194/gtes-2-55-2014>.
- [18] Nathenson M. Physical factors determining the fraction of stored energy recoverable from hydrothermal convection systems and conduction-dominated areas. In: USGS; 1975. p. 75–525. Open-file Report.
- [19] Assessment of geothermal resources of the United States. In: White DE, Williams DL, editors. USGS (1975); 1975. Circular 726.
- [20] Muffler LJP, Cataldi R. Methods for regional assessment of geothermal resources. *Geothermics* 1978;7:53–89.
- [21] Cataldi R, Lazzarotto A, Muffler P, Squarci P, Stefani G. Assessment of geothermal potential of central and southern Tuscany. *Geothermics* 1978;7:91–131.
- [22] Assessment of geothermal resources of the United States (1978). In: Muffler LJP, editor. USGS; 1979. Circular 790.
- [23] Barker BJ, Gulati MS, Bryan MA, Riedel KL. Geysers reservoir performance. In: Stone C, editor. Monograph on the Geysers geothermal field. Geothermal Resources Council; 1992. p. 167–78. Special Report No. 17.
- [24] Hickman S, Barton C, Zoback M, Morin R, Sass J, Benoit R. In-situ stress and fracture permeability in a fault-hosted geothermal reservoir at Dixie Valley, Nevada. In: Geothermal resources Council, Transactions; 1997. p. 181–9.
- [25] Sanyal SK. Forty years of production history at the Geysers geothermal field, California – the lessons learned. *Geotherm Resour Counc Trans* 2000;24:pp.317–323.
- [26] Williams CF. Development of revised techniques for assessing geothermal resources. In: *Proceedings of the 29th workshop on geothermal reservoir engineering*. Stanford University; 2004.
- [27] Blackwell DD, Negraru PT, Richard MC. Assessment of the enhanced geothermal system. Resource base of the United States. *Nat Resour Rev* 2006;15(4):283–308. <http://dx.doi.org/10.1007/s11053-007-9028-7>.
- [28] Williams CF, Reed MJ, Mariner RH. A review of methods applied by the U.S. Geological Survey in the assessment of identified geothermal resources: U.S. Geological Survey. 2008.
- [29] Beardsmore GR, Rybach L, Blackwell D, Baron C. A protocol for estimating and mapping global EGS potential, May 2011 edition, p. 11.
- [30] Zaigham NA, Nayyar ZA. Renewable hot dry rock geothermal energy source and its potential in Pakistan. *Renew Sustain Energy Rev* 2010;14(3):27. <http://dx.doi.org/10.1016/j.rser.2009.10.002>. ISSN: 1364-0321:1124–9, Open-File Report 2008-1296, <http://pubs.usgs.gov/of/2008/1296/>.
- [31] Chamorro CR, Garcia-Cuesta JL, Mondejar ME, Linares MM. An estimation of the enhanced geothermal systems potential for the Iberian Peninsula. *Renew Energy* 2014;66:1–14. <http://dx.doi.org/10.1016/j.renene.2013.11.065>. ISSN: 0960-1481.
- [32] Chamorro CR, Garcia-Cuesta JL, Mondejar ME, Perez-Madrado A. Enhanced geothermal systems in Europe: an estimation and comparison of the technical and sustainable potentials. *Energy* 2014;65:250–63. <http://dx.doi.org/10.1016/j.energy.2013.11.078>.
- [33] Feng Y, Chen X, Xu FX. Current status and potentials of enhanced geothermal system in China: a review. *Renew Sustain Energy Rev* 2014;33. <http://dx.doi.org/10.1016/j.rser.2014.01.074>. ISSN: 1364-0321:214–23.
- [34] Van Wees JD, Kramers L, Kromius A, Pluymaekers MPD, Mijnlief HF, Vis GJ. ThermoGISTM V1.0, part II: methodology. 2010. http://www.thermogis.nl/downloads/ThermoGISmanual_partII.pdf.
- [35] Geoelec project web site. 2012. Available online at: <http://www.geoelec.eu> [Last access 15/03/2015].
- [36] Van Wees JD, Boxem T, Calcagno P, Dezayes C, Lacasse C, Manzella A. A Methodology for Resource assessment and application to core countries. In: GEOELEC project, deliverable 2.1; 2013. Available on line at: <http://www>.

- geoelec.eu/wp-content/uploads/2011/09/D-2.1-GEOELEC-report-on-resource-assessment.pdf.
- [37] Montanari D, Albanese C, Catalano R, Contino A, Fedi M, Gola G, et al. Contour map of the top of the regional geothermal reservoir of Sicily (Italy). *J Maps* 2015;11(1):13–24. <http://dx.doi.org/10.1080/17445647.2014.935503>.
- [38] Di Pippo R. Ideal thermal efficiency for geothermal binary plants. *Geothermics* 2007;36:276–85. <http://dx.doi.org/10.1016/j.geothermics.2007.03.002>.
- [39] Lovekin J. Geothermal inventory. *Bull Geotherm Resour Counc* 2004;33(6):242–4.
- [40] Gola G, Manzella A, Trumphy E, Montanari D, Van Wees JD. Deep-seated geothermal resource assessment of the VIGOR project regions, Italy. In: *Proceedings of the European geothermal congress 2013 Pisa, Italy*; 2013. ISBN 978-2-8052-0226-1.
- [41] Albanese C, Allansdottir A, Amato L, Ardizzone F, Bellani S, Bertini G, et al. VIGOR: Sviluppo geotermico nelle Regioni della Convergenza. Progetto VIGOR – Valutazione del Potenziale Geotermico delle Regioni della Convergenza. In: *POI Energie Rinnovabili e Risparmio Energetico 2007–2013, Edizioni CNR – IGG Area della Ricerca di Pisa*; 2014. ISBN:9788879580113.
- [42] ENEL, ENI–AGIP, CNR, ENEA. *Inventario delle risorse geotermiche nazionali – Indagine d'insieme sul territorio nazionale*. Ministero dell'industria, del commercio e dell'artigianato (attualmente Ministero dello sviluppo economico); 1988. p. 75.
- [43] VIDEPI web site. Progetto VIDEPI, Visibilità dei dati afferenti all'attività di esplorazione petrolifera in Italia, Ministero dello Sviluppo Economico UNMIG, Società Geologica Italiana, Assomineraria. Available online at: <http://unmig.sviluppoeconomico.gov.it/videpi/> [Last access 01.12.14].
- [44] Geothopica web site. Italian national geothermal database. 2012. Available online at: <http://geothopica.igg.cnr.it/> [Last access 01/01/2014].
- [45] Trumphy E, Donato A, Gianelli G, Gola G, Minissale A, Montanari D, et al. Data integration and favourability maps for exploring geothermal systems in Sicily, southern Italy. *Geothermics* 2015;56:1–16. <http://dx.doi.org/10.1016/j.geothermics.2015.03.004>.
- [46] Cressie NAC. *Statistics for spatial data*. New York: John Wiley and Sons, Inc; 1991. p. 900.
- [47] Galgaro A, Di Sipio E, Destro E, Chiesa S, Uricchio VF, Bruno D, et al. Methodological approach for evaluating the geo-exchange potential: VIGOR Project. *AcqueSotterr. Ital J Groundw* 2012;3(130):43–53.
- [48] Warren JE, Root PJ. The behavior of naturally fractured reservoirs. *Soc Pet Engr J* 1963;3:245–55.
- [49] Gringarten AC, Sauty JP. A theoretical study of heat extraction from aquifers with uniform regional flow. *J Geophys Res* 1975;80(35):4956–62.
- [50] Augustine C. Analysis of sedimentary geothermal systems using an analytical reservoir model. *GRC Trans* 2014;38:641–7.
- [51] El-Dessouky HT, Ettouney HM. *Fundamentals of sea water desalination*. Elsevier Science B.V; 2002. p. 668.
- [52] Weber J, Bendall B, Bertani R, Bromley C, Busby J, Fujimoto K, et al. *Geothermal trend report*. 2012. p. 48.
- [53] Montanari D, Bertini G, Botteghi S, Caielli G, Caiozzi F, Catalano R, et al. Medium enthalpy geothermal systems in carbonate reservoirs, the Western Sicily example. In: *Proceedings of the European geothermal congress*; 2013. ISBN 978-2-8052-0226-1.
- [54] Trumphy E, Bertani R, Manzella A, Sander M. The web-oriented framework of the world geothermal production database: a business intelligence platform for wide data distribution and analysis. *Renew Energy* 2015;74:379–89. <http://dx.doi.org/10.1016/j.renene.2014.08.036>.
- [55] GeothermEx, Inc. *New geothermal site identification and qualification. Public interest energy research program (PIER)*. California Energy Commission; April 2004.